ELSEVIER

Journal of Molecular Catalysis A: Chemical 131 (1998) 149–156

JOURNAL OF MOLECULAR CATALYSIS A: CHEMICAL

Photocatalytic oxidation of trichloroethylene on zinc oxide: characterization of surface-bound and gas-phase products and intermediates with FT-IR spectroscopy

M.D. Driessen, T.M. Miller, V.H. Grassian *

Department of Chemistry, University of Iowa, Iowa City, IA 52242, USA

Received 7 July 1997; accepted 1 August 1997

Abstract

The gas-phase heterogeneous photooxidation of trichloroethylene (TCE) on ZnO has been investigated. In the presence of ZnO and molecular oxygen, trichloroethylene photooxidizes upon irradiation with wavelengths of light between 300 and 390 nm. Surface-bound and gas-phase products and intermediates formed during the photocatalytic oxidation of TCE were characterized with infrared spectroscopy. The gas-phase product distribution was found to be dependent on TCE pressure. At low TCE pressures, CO_2 and CO were produced as the predominant carbon-containing, gas-phase products. At high TCE pressures, additional carbon-containing products were detected. These products include phosgene, and dichloroacetylchloride. It is postulated that phosgene and dichloroacetylchloride form only after the ZnO surface becomes saturated with adsorbed products. These adsorbed photoproducts have been identified as water, bidentate formate and dichloroacetate. These adsorbed photoproducts block sites so that partial oxidation products cannot undergo further oxidation on the ZnO surface. © 1998 Elsevier Science B.V.

Keywords: Trichloroethylene; Zinc oxide; FT-IR spectroscopy

1. Introduction

Gas–solid heterogeneous photocatalytic decomposition of hazardous waste over semiconductor catalysts using solar light contains many elements of the ideal remediation process; it is energy efficient and has the potential to completely decompose molecules at ambient temperatures. As a large constituent of ground water contamination, trichloroethylene (TCE) has been the focus of many studies [1–10]. These studies have included both aqueous and gas-phase decomposition of TCE in the presence of TiO_2 and UV irradiation. TiO_2 has been the most widely studied photocatalyst because it is inexpensive, has a band gap which falls within the solar spectrum and does not undergo photodegradation [11,12]. Although some studies report that TCE completely decomposes to CO_2 and HCl [10], most other studies report the production of phosgene, an obviously undesirable toxin, and other chlorinated partial oxidation products such as dichloroacetic acid (MCAA), monochloroacetic acid (MCAA) and dichloroacetylchloride (DCAC) [1–3,5–8].

* Corresponding author. E-mail: vicki-grassian@uiowa.edu

PII S1381-1169(97)00262-8

A photocatalyst with a similar bandgap, but one which does not form these toxic byproducts, would be highly desirable and an improvement over current technology. ZnO is a possible candidate that has a similar band gap (3.2 eV) and has shown to be, in some cases, a more active photocatalyst [11,12]. Even more importantly, ZnO may possess a selectivity for complete mineralization of chlorinated waste.

Herein we report on the photooxidation of TCE on ZnO. In the presence of ZnO and molecular oxygen, TCE photooxidizes upon irradiation with light of wavelengths between 300 and 440 nm. Fourier transform infrared spectroscopy is used to characterize surface-bound and gas-phase products and intermediates formed in the reaction. It is shown that the gas-phase product distribution for this reaction is dependent on the reaction conditions. CO_2 and CO are formed during TCE photooxidation on ZnO for all TCE pressures investigated. At high TCE pressures, additional products are formed. These products include phosgene and dichloroacetylchloride. It is postulated that under conditions of higher pressures, the surface becomes saturated with adsorbed products that block sites for the continued oxidation of phosgene and dichloracetylchloride. These surface-bound products are identified by infrared spectroscopy as adsorbed water, bidentate formate and dichloroacetate.

2. Experimental section

The apparatus used in these experiments has been described previously [13,14]. Briefly, it consists of an all stainless steel vacuum system with an infrared cell made from a stainless steel cube. The entire system is pumped by an 80 l/s ion pump and rough pumped using a turbomolecular pump.

Samples are made by spraying a slurry of ZnO (Aldrich, Reagent Grade-surface area of $\sim 5\ m^2/g$) in deionized water onto a tungsten grid (Buckbee–Mears) which is held at approximately 573 K. A template is used to mask half of the grid so that one side can be coated with ZnO and the other is left blank so that gas-phase species can be monitored during irradiation with infrared spectroscopy. Approximately 60 mg of ZnO are coated onto a 3 cm × 1 cm area of the grid for the infrared experiments and about 150 mg are coated onto the entire grid surface (3 cm × 2 cm) for the mass spectral experiments.

After the sample is prepared, it is mounted inside of the sample cell after which the cell is evacuated. The sample is then resistively heated to 673 K for 2.5 h under vacuum and then oxidized at the same temperature by introducing 100 Torr of O_2 into the IR cell for 30 min. After evacuating the sample cell for 15 min, 100 Torr of oxygen is admitted into the cell and the sample is cooled to room temperature. Once the sample has reached room temperature, the cell is evacuated for several hours or overnight.

The IR cell is then placed on a linear translator inside the sample compartment of the Mattson RS-1 FT-IR spectrometer equipped with a narrowband MCT detector. Each spectrum was recorded by averaging 1000 scans at an instrument resolution of 4 cm^{-1}. Each absorbance spectrum shown represents a single beam scan referenced to the appropriate single beam scan of freshly processed ZnO or the blank grid prior to adsorption, unless otherwise noted.

A DetecTorr II (UTI) quadrupole mass spectrometer, housed in a high vacuum chamber pumped by a 400 l/s ion pump, is used to detect gas-phase products. The stainless steel cube was connected to the mass spectrometer chamber through a calibrated leak valve.

The light from a 200 W high pressure mercury lamp (Oriel) was passed through both a water and 300-nm broad band filter before it was reflected off of an aluminum coated mirror and onto a quartz prism mounted inside the FT-IR sample compartment. The quartz prism is mounted inside of the FT-IR sample compartment so that the dry N_2 purge was not broken during irradiation. The light from the quartz prism was then directed onto the ZnO catalyst.

The power at the sample was measured before each experiment and was typically 80 mW/cm^2. The temperature of the sample did not exceed 315 K during irradiation.

For the wavelength dependence study, several long pass Oriel filters were used. The stated cut-off (0% transmission below the stated wavelength) and the corresponding fraction of the full arc power that the filter delivered are: #59460, $\lambda > 330$ nm—0.82; #59472, $\lambda > 385$ nm—0.70; #59484, $\lambda > 440$ nm—0.54; #59492, $\lambda > 475$ nm—0.51.

TCE (Aldrich) and DCAC (Aldrich) with a stated purity of 99 + % and 99%, respectively, were transferred to a glass sample bulb and subjected to several freeze–pump–thaw cycles before use. Oxygen (Air Products) with a stated purity of 99.6% was used as received.

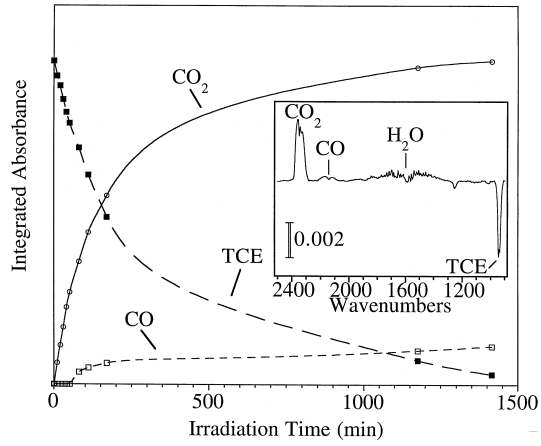

Fig. 1. Integrated area of infrared bands associated with TCE and gas-phase products plotted as a function of irradiation time: TCE (940 cm^{-1}), CO (2144 cm^{-1}) and CO_2 (2349 cm^{-1}). The inset shows the difference infrared spectrum following the nearly complete photooxidation of 144 mTorr of TCE. For the difference spectrum, the initial gas-phase spectrum of reactants has been subtracted from the gas-phase spectrum taken following irradiation.

3. Results and discussion

3.1. TCE photooxidation on ZnO at low TCE pressures

Initial experiments were done to determine if there was any reaction between TCE, O_2 and ZnO in the absence of light. A gas mixture of 144 mTorr TCE and 721 mTorr O_2 was allowed into the IR cell in the presence of ZnO. After 30 min, infrared spectra were taken of both the ZnO sample and the gas phase. It was found that no reaction occurred without the presence of the light.

This same mixture was irradiated and Fig. 1 displays a plot showing the decrease in integrated area of gas-phase TCE (940 cm^{-1} band) and the increase in integrated area of gas-phase product absorption bands as a function of irradiation time. As the plot shows, the growth of CO_2 (2349 cm^{-1} band) mirrors the consumption of TCE. CO (2144 cm^{-1} band) has an induction period and then begins to grow in. The increase in production of gas-phase water is not plotted, due to the difficulty in quantifying the amount of water produced, since a large amount adsorbs on the ZnO surface (vide infra). Complete photooxidation of 144 mTorr of TCE is accomplished after approximately 1500 min. The inset in Fig. 1 shows the difference in gas-phase infrared spectrum after nearly complete conversion of TCE. The negative feature near 940 cm^{-1} is associated with the consumption of TCE and the positive features are associated with the gas-phase products CO, CO_2 and H_2O.

The wavelength dependence of the photooxidation of TCE on ZnO was investigated. Fig. 2 shows a plot of the integrated area of the infrared band for CO_2 as a function of the wavelength used during irradiation. Starting with the longest wavelength filter first, the ZnO photocatalyst was irradiated for 10 min in the presence of TCE (144 mTorr) and O_2 (721 mTorr). The next longest wavelength filter was then put in place and irradiation was continued for an additional 10 min. This procedure was followed for all five filters used in this experiment. The increase in the integrated area of the CO_2 infrared band after irradiation with each filter was then corrected for the differences in light output

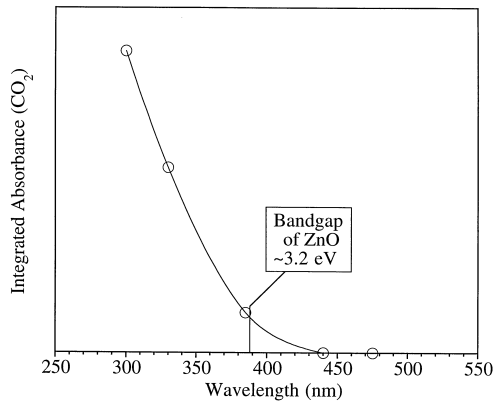

Fig. 2. Wavelength dependence of TCE photooxidation over ZnO. The infrared band for CO_2 (2349 cm^{-1}) was integrated and plotted as a function of wavelength after normalizing for differences in the lamp output for the different cut-off filters.

between filters. As can be seen in Fig. 2, the onset wavelength of CO_2 production coincides with the bandgap of ZnO. Irradiation at shorter wavelengths, i.e., photon energy above the bandgap results in an even greater amount of CO_2 production. The wavelength dependence indicates that the photooxidation of TCE is initiated by the excitation of ZnO and not by direct absorption of TCE, which absorbs UV light with $\lambda < 276$ nm.

Gas-phase products from the photooxidation of TCE on ZnO at low pressures (144 mTorr TCE/721 mTorr O_2) were monitored using mass spectrometry as well. The reaction gas mixture was sampled by opening the leak valve from the reaction cell to the mass spectrometer at a constant leak rate during irradiation. Fig. 3 displays a 'difference' residual gas analysis scan from $m/e = 1$ to 200 after 227 min of irradiation. The background spectrum of initial gas phase reactants (before irradiation) has been subtracted from the mass spectrum taken after irradiation to show newly formed gas phase products and the loss of reactants. All of the negative features (downward lines) are associated with the consumption of TCE except for the negative feature at $m/e = 32$ due to the consumption of molecular oxygen. Several of the positive features in the 'difference' mass spectrum are associated with the same major products observed in the infrared spectrum namely, H_2O ($m/e = 18$), CO ($m/e = 28$) and CO_2 ($m/e = 44$). Two products observed in the mass spectral data that are not as apparent in the infrared data are HCl ($m/e = 36, 38$) and $CHCl_3$ ($m/e = 83, 85$). Multiple peaks in the mass spectrum for these species are due to the two chlorine isotopes, ^{35}Cl and ^{37}Cl. Phosgene and DCAC are not detected, in agreement with the IR data.

In the presence of broadband irradiation, changes in the infrared spectrum of the ZnO surface are seen after 10 min. The infrared spectra in the region extending from 1000 to 4000 cm^{-1} of adsorbed species following broadband irradiation ($\lambda > 300$ nm) of 144 mTorr TCE and 721 mTorr O_2 are shown in Fig. 4 as a function of irradiation time. After 10 min of broadband irradiation, species adsorbed on ZnO have infrared absorption bands at 2883, 2790, 1606, 1575, 1424, 1379, 1362 and 1232 cm^{-1}. After 30 min of irradiation, all of the bands near 2883, 2790, 1606, 1575, 1424, 1379 and 1362 cm^{-1} have increased in intensity and are accompanied by the growth of several new bands near 3335, 3015 and 1620 cm^{-1}. Although initially less intense, the absorption bands

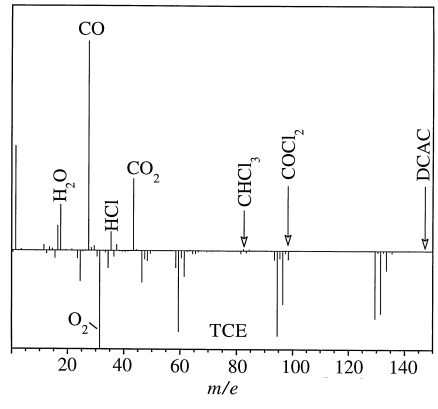

Fig. 3. A difference mass spectrum ($m/e = 1$ to 200) after 227 min of irradiation of TCE and ZnO (see text for reaction conditions). The mass spectrum of the reactants has been subtracted from the mass spectrum acquired following irradiation. All of the negative features (downward lines) are due to TCE consumption except for the feature at $m/e = 32$ due to O_2 consumption.

near 1606 and 1424 cm^{-1} become more intense relative to the absorption bands near 1575, 1379 and 1362 cm^{-1} after 40 min of irradiation.

Based on literature frequencies and assignments, the bands in the infrared spectra shown in Fig. 4 can be assigned to several surface-bound products. The surface species present after the first 10 min of irradiation has an infrared spectrum with absorptions near 2883, 2790, 1575, 1379 and 1362 cm^{-1}. These absorptions are characteristic of bidentate formate, $HCOO^-$ (Table 1) [15]. The set of bands near 1620 and 3355 cm^{-1} are assigned to the bending mode and the OH stretch of adsorbed water, respectively [16]. A third surface product which is formed during irradiation has absorption bands with frequencies of 3015, 1606, 1424 and 1232 cm^{-1}, these bands are characteristic of an adsorbed carboxylate, $RCOO^-$ [17]. These remaining absorption bands can be assigned to dichloroacetate, as discussed in more detail in Section 3.2.

Losses in the hydroxyl region for isolated OH groups (ZnOH) at 3615 and 3672 cm^{-1} occur simultaneously with water adsorption. This may be due to hydrogen bonding between OH groups and adsorbed water and/or to the loss of OH groups on the ZnO surface during the photooxidation reaction.

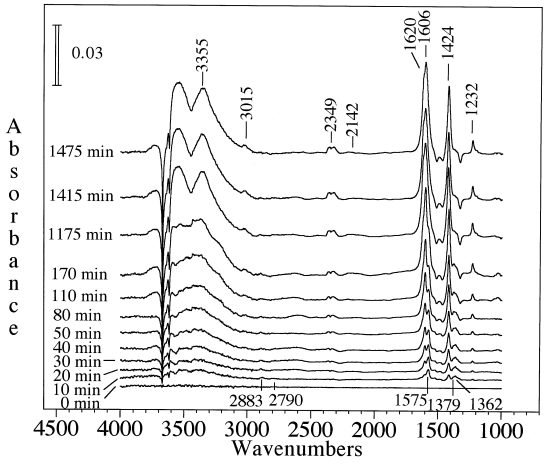

Fig. 4. Infrared spectra of the ZnO surface as a function of irradiation (144 mTorr TCE/721 mTorr O_2). Infrared absorptions of gas phase and adsorbed species due to TCE parent absorptions have been subtracted out from the spectra so that only absorption bands due to gas phase products (CO—2144 cm^{-1}; CO_2—2349 cm^{-1}) and adsorbed products (bidentate formate, dichloroacetate and water—see Table 1 for band assignments) are present in the spectra.

Table 1
Vibrational assignment of adsorbed species on ZnO

I. Bidentate formate, $HCOO^-$	
Photoproduct bands from TCE photooxidation[a]	Bidentate formate[b], HCOO on ZnO
–	2960, $\nu(COO^-)+\delta(CH)$
2883	2882, $\nu(CH)$
2790	2740, $\nu_s(COO^-+\delta(CH)$
1575	1580, $\nu_a(COO^-)$
1379	1382, $\delta(CH)$
1362	1365, $\nu_s(COO^-)$
II. Water, H_2O	
Photoproduct bands from TCE photooxidation[a]	Adsorbed water[c]
1620	1610, $\delta(H_2O)$
3355	3450, $\nu(OH)$
III. Dichloroacetate, Cl_2HCCOO^-	
Photoproduct bands from TCE photooxidation[a]	Dichloroacetate on ZnO[d]
3015	3015, $\nu(CH)$
1609	1605, $\nu_{as}(COO^-)$
1426	1427, $\nu_s(COO^-)$
1232	1232, $\delta(CH)$
965	[e], $\nu(CC)$
830	831, $\nu_{as}(CCl_2)$
791	792, $\nu_s(CCl_2)$

[a] This work.
[b] Ref. [15].
[c] Ref. [16].
[d] This work, from reaction of DCAC and ZnO.
[e] Hidden under a broad absorption band near goo^{-1} cm that is unassigned.

3.2. TCE photooxidation on ZnO at high TCE pressures

The results in Section 3.1 show that the predominant carbon-containing products in the photooxidation of 144 mTorr of TCE on ZnO are CO_2 and CO. At higher pressures, TCE conversion decreases, and there is the appear-

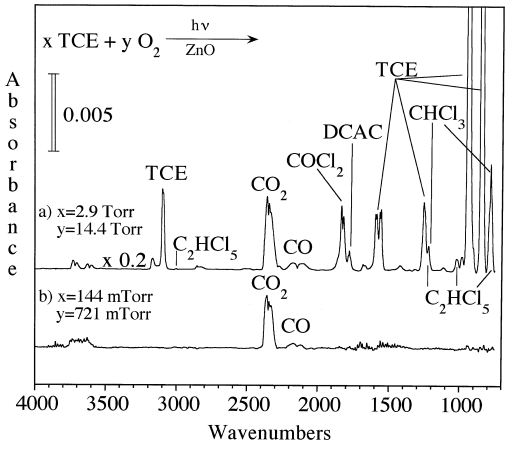

Fig. 5. Infrared spectrum recorded of the gas-phase products after photooxidation of TCE on ZnO (a) after irradiation of 2.9 Torr of TCE and 14.4 Torr of oxygen (TCE:O_2 = 1:5) for 28.5 h; (b) after irradiation of 144 mTorr of TCE and 721 mTorr of oxygen (TCE:O_2 = 1:5) for 24.5 h. Product bands are observed at 1827 cm^{-1} ($COCl_2$); 2349 cm^{-1} (CO_2); 2144 cm^{-1} (CO); 1790 cm^{-1} (DCAC); 1220 and 776 cm^{-1} ($CHCl_3$); and 3001, 1215, 1026 and 778 cm^{-1} (C_2HCl_5) [2].

ance of additional gas-phase products. [1] The infrared spectrum recorded of the gas-phase after photooxidation of 2.9 Torr of TCE on ZnO in the presence of 14.4 Torr of O_2 (TCE:O_2 = 1:5) is shown in Fig. 5a. For comparison, the infrared spectrum recorded of the gas phase after photooxidation of 144 mTorr of TCE on ZnO in the presence of 721 mTorr of O_2 (TCE:O_2 = 1:5) is shown in Fig. 5b. The infrared spectrum after photooxidation of 2.9 Torr of TCE (Fig. 5a) clearly shows that not all of the TCE is converted after 28.5 h of irradiation. The spectrum also shows the formation of additional gas-phase products. These products include phosgene, DCAC, chloroform and pentachloroethane. [2]

The infrared spectrum recorded of the ZnO surface after photooxidation of TCE at the higher pressures is shown in Fig. 6a. Adsorbed product are observed on the ZnO surface with absorptions at 3350, 3015, 1790, 1620, 1606, 1425, 1232, 965, 830 and 790 cm^{-1}. There are some similar surface-bound products detected after photooxidation of TCE at a pressure of 2.9 Torr compared to photooxidation of 144 mTorr of TCE after 1475 min (Fig. 4). However, the absorption bands are approximately three times greater in intensity for the reaction done at higher pressures.

It has been recently determined from NMR studies that the predominant carbon-containing, surface-bound product from TCE photooxidation on Degussa P25 TiO_2 is dichloroacetate [18]. It was postulated that dichloroacetate formed from the reaction of dichloroacetyl chloride and hydroxyl groups to yield HCl and dichloroacetate. The IR spectrum of the ZnO surface following TCE photooxidation at high pressures is consistent with an adsorbed carboxylate. In order to confirm that dichloroacetate is a surface-bound photoproduct, the surface chemistry of DCAC on ZnO was investigated.

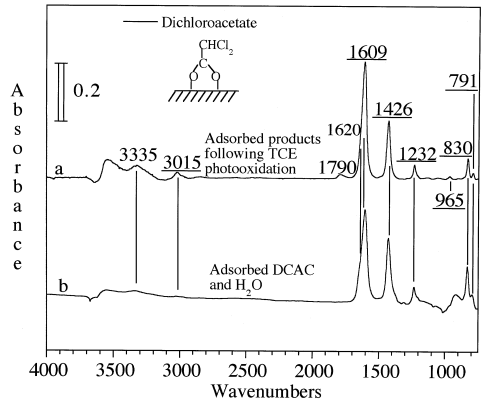

Fig. 6. Infrared spectra recorded of the ZnO surface (a) after photooxidation of 2.9 Torr of TCE with O_2 (14.4 Torr). The intensity of the infrared absorption bands for adsorbed products at the higher TCE pressure is nearly a factor of ten greater than that observed at lower pressures (see Fig. 4). Nearly all of the bands in the spectrum can be assigned to dichloroacetate and adsorbed water. The band near 1790 cm^{-1}, only observed after photooxidation of high pressures of TCE, is assigned to the C=O stretch of an adsorbed carbonyl, most likely adsorbed phosgene. (b) Infrared spectrum recorded after reaction of DCAC on the ZnO surface to give adsorbed dichloroacetate, this surface was then exposed to water vapor.

[1] A 500 W Hg Arc lamp was used for the high pressure TCE experiments, to get a larger percent conversion of TCE.

[2] Some of the pentachloroethane absorption bands are hidden under the more intense TCE parent absorption bands and others overlap with chloroform absorption bands.

The infrared spectrum recorded following reaction of DCAC on a clean ZnO surface is shown in Fig. 6. DCAC was introduced into the IR cell at a pressure of 0.500 Torr and then evacuated. Water, another product of the TCE photooxidation reaction, was adsorbed subsequently on the surface at a pressure of 0.5 Torr followed by evacuation. The spectrum shown in Fig. 6b was taken after evacuation of gas-phase water. The two spectra shown in Fig. 6, the photoproduct spectrum and the DCAC/H_2O spectrum, are nearly identical and show that dichloroacetate is a surface-bound product formed during TCE photooxidation. There is an additional weaker band at 1790 cm^{-1} present in the spectrum shown in Fig. 6 that is not present in the spectrum shown in Fig. 4. This band can be assigned to the C=O stretch of an adsorbed carbonyl on the ZnO surface, most likely adsorbed phosgene [8].

3.3. Photooxidation mechanism and the role of adsorbed products

From the data presented here, it has been shown that in the presence of molecular oxygen, ZnO is an effective photocatalyst in the oxidation of TCE with wavelengths of light between 300 and 440 nm. The infrared spectral data show that at low pressures, the photooxidation of TCE is complete and the major carbon-containing, gas-phase products are CO_2 and CO. Surface-bound species on the ZnO photocatalyst surface have been identified as water, bidentate formate and dichloroacetate. Most importantly, under the low pressure conditions, there is no evidence for the production of phosgene or any other toxic partial oxidation products (e.g., MCAA, DCAA or DCAC). At higher pressures of TCE, chlorinated partial oxidation products are formed. Phosgene and DCAC are apparent in the infrared spectrum. $CHCl_3$ and C_2HCl_5 are also identified as a major product. The main difference between the reactions done at high pressure and those done at low pressure is that the ZnO surface becomes saturated with photoproducts at the higher TCE pressures. Therefore, surface reactions are inhibited due to site-blocking. The blocking of sites leads to a decrease in the formation of more complete oxidation products, CO and CO_2, relative to partial oxidation products such as phosgene.

Recently, Fan and Yates [8] have presented strong evidence to show that the active species in the gas-phase photooxidation of TCE on TiO_2 is molecular oxygen and not OH groups or adsorbed water. Similarly, we have shown here that molecular oxygen is consumed in the reaction (see difference mass spectral data shown in Fig. 3) and is therefore an active participant in the photooxidation of TCE on ZnO. ZnO and TiO_2 are both semiconductors with similar bandgaps (3.2 eV). It is then reasonable to extend the findings concerning the active species found for the photooxidation of TCE on TiO_2 to the photooxidation of TCE on ZnO. Therefore, it is proposed that ZnO produces a similar excited adsorbed oxygen species that is active in the photooxidation of TCE.

There is some discrepancy in the literature concerning the product distribution in the photooxidation of TCE on TiO_2. In another publication, we will report on the factors that influence the product distribution for TCE photooxidation on TiO_2. These factors include TCE pressure, O_2 pressure and the presence of adsorbed products on the TiO_2 surface [19]. Our data for TiO_2 show that similar to what is observed here, the gas-phase product distribution is dependent on the coverage of adsorbed products in that adsorbed products block sites so that surface reactions are inhibited.

4. Conclusions

FT-IR spectroscopy has been used to identify gas-phase and surface-bound products and intermediates in the photocatalytic oxidation of TCE on ZnO. The product distribution for TCE photooxidation on ZnO is shown to change depending on reaction conditions. At high TCE

pressures, when the surface of the ZnO photocatalyst is saturated with adsorbed products, partial oxidation products such as phosgene and DCAC form. This study shows that adsorbed products on the photocatalyst surface strongly influence product distribution.

Acknowledgements

The authors gratefully acknowledge the National Science Foundation (Grant CHE-9614134).

References

[1] M.R. Nimlos, W.A. Jacoby, D.M. Blake, T.A. Milne, Photocatalytic purification and treatment of water and air, in: D.F. Ollis, H. Al-Ekabi (Eds.), Trace Met. Environ. 3, Elsevier, 1993, p. 387.
[2] W.F. Jardim, R.M. Alberici, M.M.K. Takiyama, C.P. Huang, Hazard. Ind. Wastes 26 (1994) 230.
[3] W.A. Jacoby, M.A. Nimlos, D.M. Blake, R.D. Noble, C.A. Koval, Environ. Sci. Technol. 28 (1994) 1661.
[4] N.N. Lichtin, M. Avudaithai, Environ. Sci. Technol. 30 (1996) 2014.
[5] S. Yamazaki-Nishida, S. Cervera-March, K.J. Nagano, M.A. Anderson, K. Hori, J. Phys. Chem. 99 (1995) 15814.
[6] J.F. Kenneke, J.L. Ferry, W.H. Glaze, Photocatalytic purification and treatment of water and air, Trace Met. Environ. 3 (1993) 179.
[7] S.A. Larson, J.L. Falconer, Photocatalytic purification and treatment of water and air, Trace Met. Environ. 3 (1993) 473.
[8] J. Fan, J.T. Yates Jr., J. Am. Chem. Soc. 118 (1996) 4686.
[9] J.S. Wong, A. Linsebigler, G. Lu, J. Fan, J.T. Yates Jr., J. Phys. Chem. 99 (1995) 335.
[10] G.B. Raupp, L.A. Dibble, PCT Int. Appl., US 89-407573 890915 (Patent).
[11] N. Serpone, E. Pelizzetti (Eds.), Photocatalysis, Fundaments and Applications, Wiley, New York, 1989.
[12] H. Hidaka, K. Nohara, K. Ooishi, J. Zhao, N. Serpone, E. Pelizzetti, E. Chemosphere 29 (1994) 2619.
[13] P. Basu, T.H. Ballinger, J.T. Yates Jr., Rev. Sci. Instr. 59 (1988) 1321.
[14] J. Fan, J.T. Yates Jr., J. Phys. Chem. 98 (1994) 10621.
[15] C. Chauvin, J. Saussey, J.-C. Lavalley, H. Idriss, J.-P. Hindermann, A. Kiennemann, P. Chaumette, P. Courty, J. Catal. 121 (1990) 56.
[16] L.H. Little, Infrared Spectra of Adsorbed Species, Academic Press, London, 1966, p. 76.
[17] A.A. Davydov, Infrared Spectroscopy of Adsorbed Species on the Surface of Transition Metal Oxides, Wiley, Chichester, 1990, p. 148.
[18] S.-J. Hwang, C. Petucci, D. Rafterty, J. Am. Chem. Soc. 119 (1997) 7877.
[19] M.D. Driessen, V.H. Grassian, J. Phys. Chem. B (in press).